Supplementary figure 1

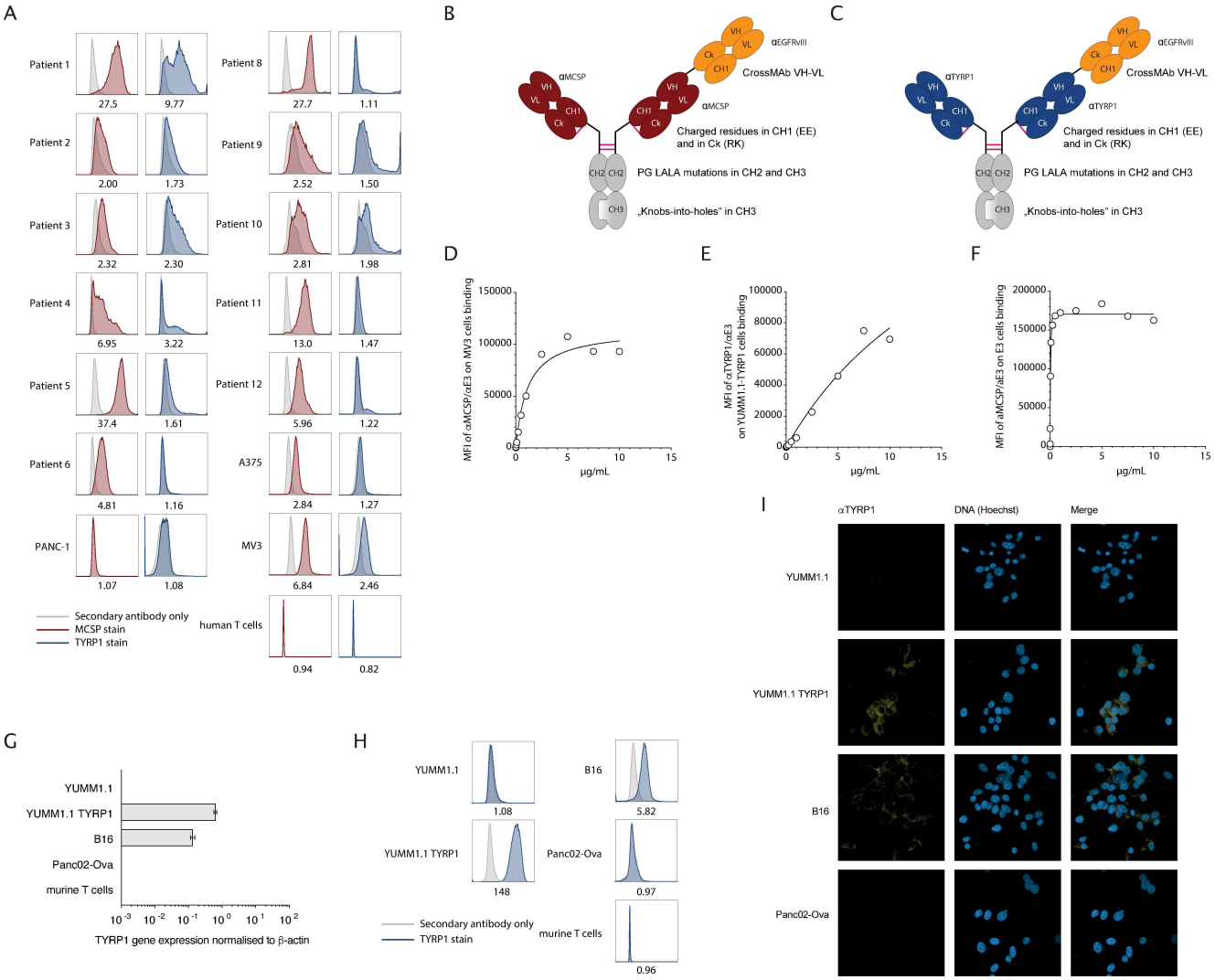

Supplementary figure 2

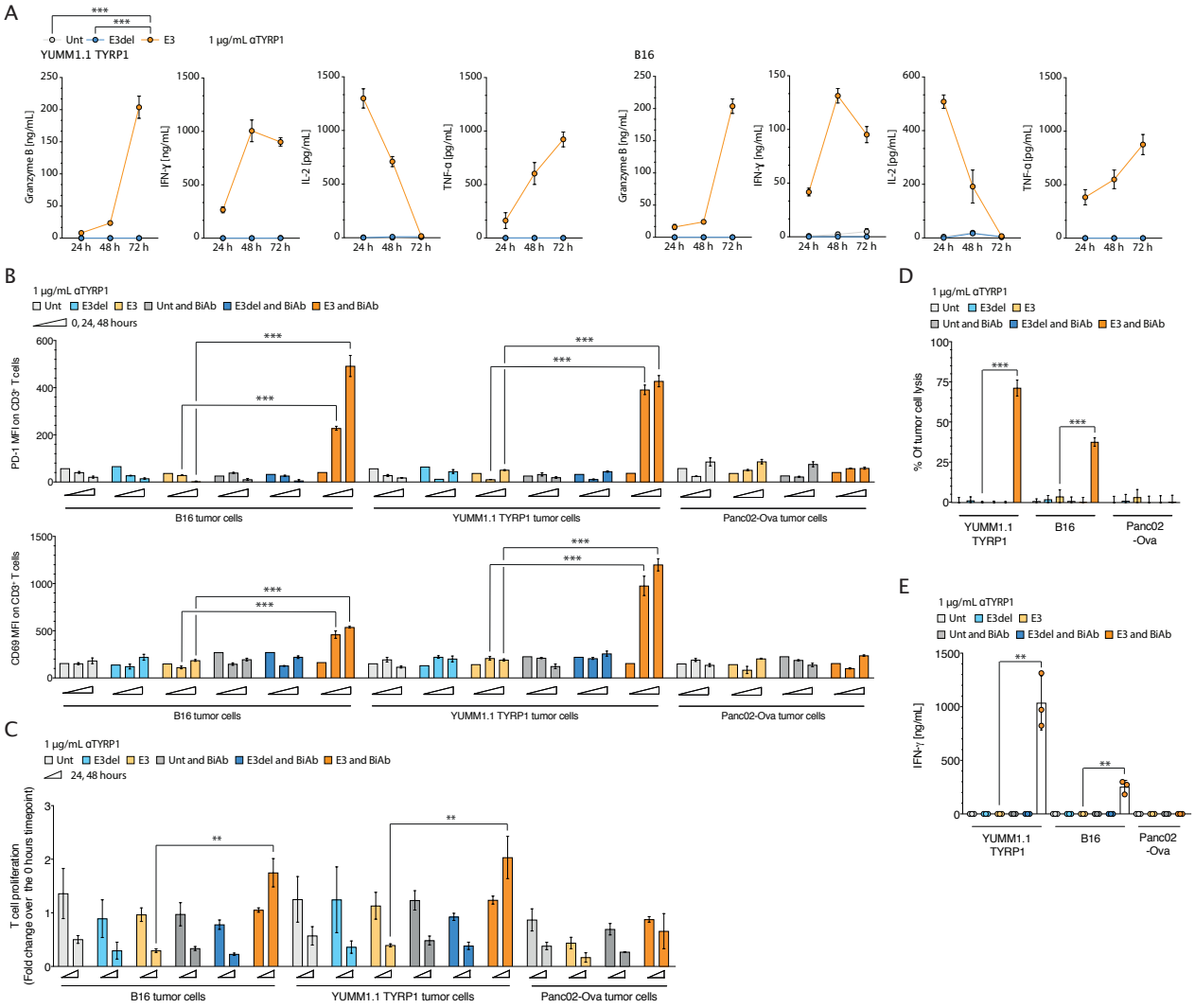

Supplementary figure 3

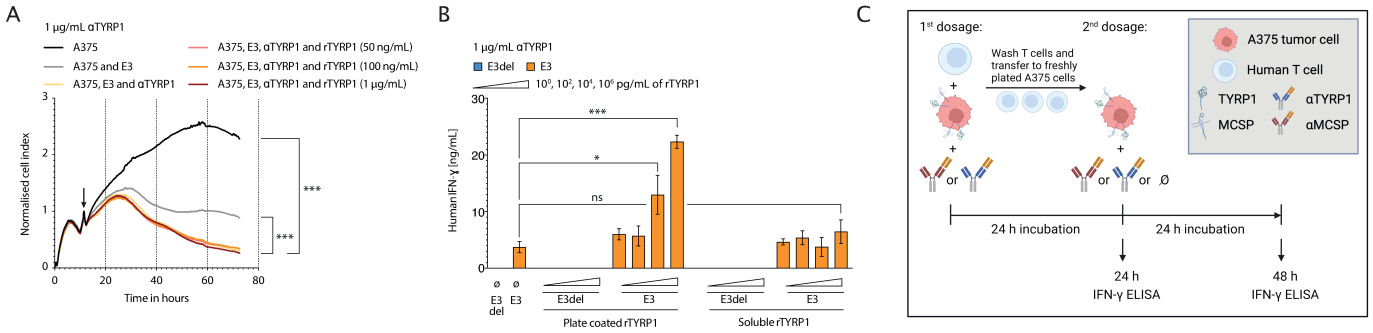

Supplementary figure 4

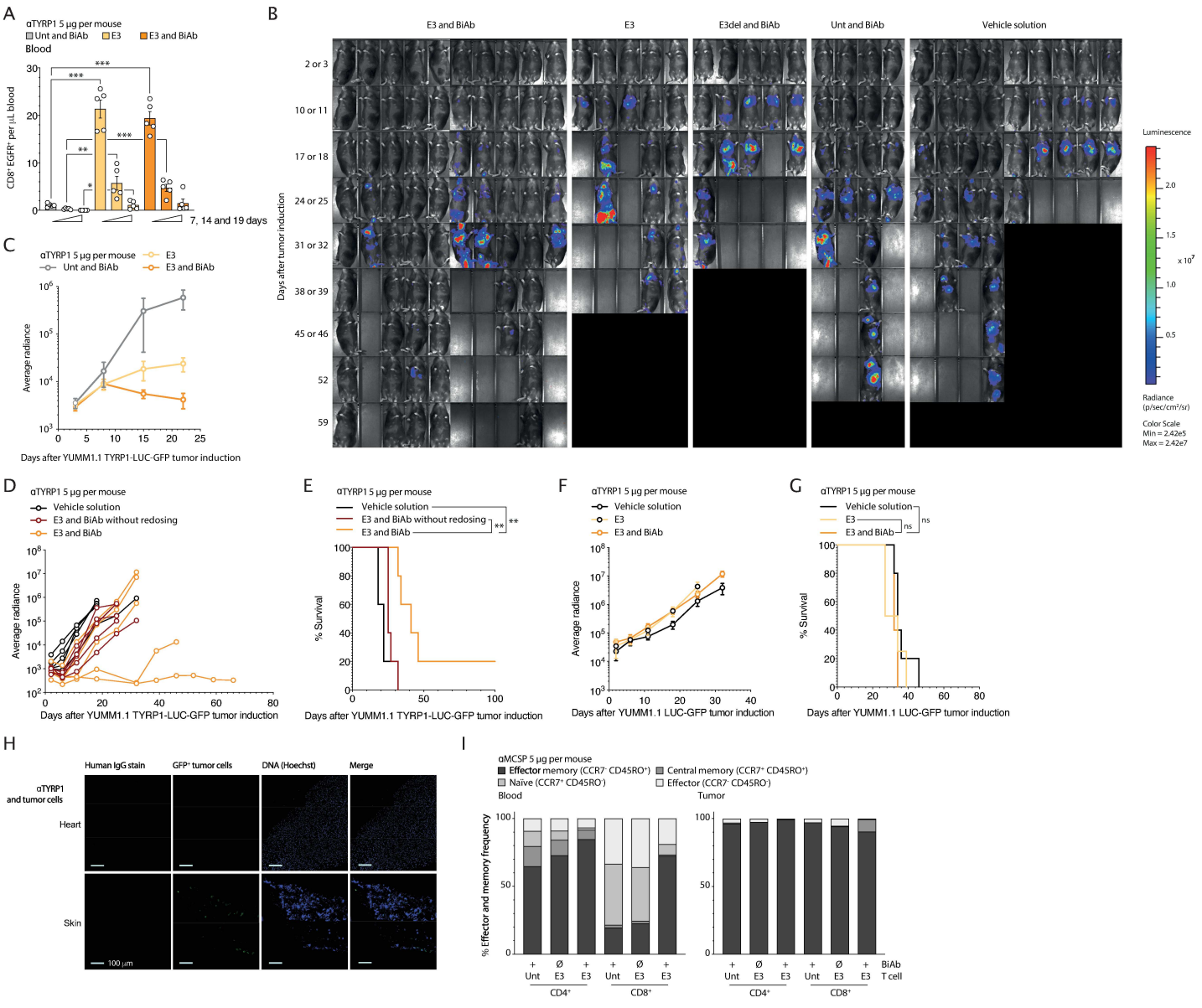

Supplementary figure 1: MCSP and TYRP1 expression on patient-derived melanoma samples, human and murine melanoma cell lines, structure and binding properties of αTYRP1/αE3 and αMCSP/αE3 BiAb. A) MCSP and TYRP1 protein expression was assessed with either one of the BiAb (human IgG1) and anti-human IgG secondary antibody. Median fluorescence intensity (MFI) ratio of MCSP or TYRP1 stain and secondary antibody only stain was depicted below each flow cytometry plot. B) and C) Schematic drawing of the αMCSP/αE3 BiAb molecule in (B) and the αTYRP1/αE3 in (C). VL and VH, variable domain of immunoglobulin (Ig) light or heavy chain. CK, constant domain of Ig light chain kappa. CH1/2/3, first/second/third constant domain of Ig heavy chain. E, R, K, P, G, L, A, amino acids. D-F) Dissociation constant (K_D) determination of BiAb modules. Binding to MCSP in (D) (K_D = 1.1 μg/mL), TYRP1 in (E) (K_D = 18 μg/mL), and EGFRvIII in (F) (K_D = 42 ng/mL) on MV3, YUMM1.1 TYRP1 or E3 SAR T cells, as measured by flow cytometry. G) RT-PCR TYRP1 gene analysis of murine cell lines, and murine T cells. H) TYRP1 protein expression was assessed with αTYRP1/αE3 BiAb (human IgG1) and anti-human IgG secondary antibody. I) Microscopic analysis of TYRP1 expression on permeabilized YUMM1.1, YUMM1.1 TYRP1, B16 and Panc02-Ova cells using αTYRP1/αE3 BiAb (αTYRP1) and anti-human IgG secondary antibody. Experiments show mean values of two biological experiments for (D), (E) and (F), one experiment for (A), and (H). Experiments in subfigure (G) show mean values ± SD calculated from 3 technical replicates and one representative of two independent experiments in subfigure (I).

Supplementary figure 2: αTYRP1/αE3 BiAb activates SAR T cells to mediate specific cytotoxicity against murine melanoma cell lines. A) ELISA for granzyme B, IFN-γ, IL-2 and TNF-α on supernatant of murine T cells in coculture with murine melanoma cell lines YUMM1.1 TYRP1 or B16 (E:T 2:1) and αTYRP1/αE3 BiAb (αTYRP1, 1 μg/mL). Supernatant was taken after 24, 48 and 72 hours (n = 3). B) Frequency of PD-1 and CD69 expression on

T cells after 0, 24 and 48 hours of coculture with murine melanoma cell lines YUMM1.1 TYRP1, B16 or murine pancreatic cancer cell line Panc02-Ova (E:T 2:1) and αTYRP1/αE3 BiAb (1 µg/mL) (n = 3). C) Following 48 hours of coculture the $CD3^+$ T cell count was assessed using a flow cytometry-based readout and normalized to the 0 hour conditions (n = 3). D) The percentage lysis of melanoma cell lines YUMM1.1 TYRP1, B16 and Panc02-Ova mediated via αTYRP1/αE3 BiAb and SAR T cells. The cytotoxicity was assessed with a LDH assay after 48 hours of coculture (n = 3). E) ELISA for IFN-γ on supernatant of murine T cells in coculture with murine melanoma cell lines YUMM1.1 TYRP1, B16 or Panc02-Ova (E:T 2:1) and αTYRP1/αE3 BiAb (αTYRP1, 1 µg/mL). Statistical analysis was performed using the unpaired two-tailed Student's t test. Statistics shown in (A) were calculated based on the 24 hour time points. Experiments show mean values ± SD calculated from 3 biological replicates and are representative of three independent experiments (A, B, D and E) and mean values ± SEM calculated from n independent biological replicates (C).

Supplementary figure 3: Modular, selective and reversible activation of SAR T cells, irrespective of soluble forms of TYRP1 tumor antigen. A) A375 melanoma cells were plated and cocultured with human SAR T cells (E:T 2:1) and αTYRP1/αE3 BiAb (αTYRP1, 1 µg/mL). Different concentrations of soluble, recombinant TYRP1 (rTYRP1) were added. The tumor cell lysis over time was assessed using xCELLigence (n = 3). The cell index was normalized to the respective time point of T cell addition as indicated by an arrow. B) Human SAR or E3del control T cells and αTYRP1/αE3 BiAb (1 µg/mL) were plated in wells that were either coated with different concentrations of rTYRP1 or where different concentrations of soluble rTYRP1 were added to the medium. After 48 hours the supernatant was taken and analyzed for IFN-γ using ELISA (n = 3). C) Schematic overview of the assay setup from experiments in Figure 4 (D) and (E). Analyses of differences between groups for (A) were performed using two-way ANOVA with correction for multiple testing by the Bonferroni

method. For statistical analysis of (B), the unpaired two-tailed Student's t test was used. Experiments show mean values ± SD calculated from 3 biological replicates and are representative of three independent experiments.

Supplementary figure 4: Treatment with the SAR T cell-BiAb combination is effective in syngeneic and xenograft melanoma models. A) The murine $CD8^+$ SAR T cell persistence per μL blood was analyzed using flow cytometry 7, 14 and 19 days after T cell transfer. The mice were treated according to the experiment in Figure 5 (C). B) *In vivo* imaging data of Figure 5 (A) displaying luminescent signal in radiance for all experimental groups two or three days after YUMM1.1 TYRP1-LUC-GFP tumor induction onwards (days 2/3, 10/11, 17/18, 24/25, 31/32, 38/39, 45/46, 52 and 59). C) YUMM1.1 TYRP1-LUC-GFP tumor growth curves of experiment depicted in Figure 5 (C) based on *in vivo* luminescent signal imaging (days 3, 8, 15 and 22). D) YUMM1.1 TYRP1-LUC-GFP tumor growth curves based on *in vivo* luminescent signal imaging (days 2, 6, 11, 18, 25, 32, 39 and 45; for each group n = 5). The mice were treated according to the experiment in Figure 5 (A) with either SAR T cells and αTYRP1/αE3 BiAb (redosed twice per week), SAR T cells and αTYRP1/αE3 BiAb (one dose) or the vehicle solution (for all groups: n = 5). E) Percentage survival readout. F) YUMM1.1 LUC-GFP tumor growth curves based on *in vivo* luminescent signal imaging (days 2, 6, 11, 18, 25 and 32). The mice were treated according to the experiment in Figure 5 (A) with either SAR T cells and αTYRP1/αE3 BiAb (redosed twice per week) (n = 5), SAR T cells (n = 4), or the vehicle solution (n = 5). The experiment was simultaneously conducted with the experiment depicted in Supplementary Figure 4D. G) Percentage survival readout. H) Immunofluorescence imaging of the αTYRP1/αE3 BiAb and tumor cell-derived GFP in heart and skin tissue of tumor bearing mice injected with the αTYRP1/αE3 BiAb. The mice were treated according to the experiment in Figure 5 (D). I) Frequency of effector memory ($CCR7^-$ and $CD45RO^+$), central memory ($CCR7^+$ and

CD45RO$^+$), naïve (CCR7$^+$ and CD45RO$^-$) and effector (CCR7$^-$ and CD45RO$^-$) phenotype on human CD4$^+$ and CD8$^+$ T cells in blood and tumor 14 days after T cell transfer. For statistical analysis of (A), the unpaired two-tailed Student's t test was used. For statistical analysis of survival data, the log-rank test was applied. Experiments show mean values ± SEM calculated from n biological replicates, one experiment for (A), (D), (E), (F), (G), (H) and (I) and one representative of two independent experiments in (B) and (C).